Enhanced potency of a fucose-free monoclonal antibody being developed as an Ebola virus immunoprotectant

Larry Zeitlin[a,1], James Pettitt[b], Corinne Scully[b], Natasha Bohorova[a], Do Kim[a], Michael Pauly[a], Andrew Hiatt[a], Long Ngo[c], Herta Steinkellner[d], Kevin J. Whaley[a], and Gene G. Olinger[b]

[a]Mapp Biopharmaceutical, San Diego, CA 92121; [b]Department of Virology, US Army Medical Research Institute of Infectious Diseases, Frederick, MD 21702; [c]Department of Medicine, Beth Israel Deaconess Medical Center, Boston, MA 02215; and [d]Department of Applied Genetics and Cell Biology, University of Natural Resources and Life Sciences, 1190 Vienna, Austria

Edited* by Charles J. Arntzen, Arizona State University, Tempe, AZ, and approved July 28, 2011 (received for review May 25, 2011)

No countermeasures currently exist for the prevention or treatment of the severe sequelae of Filovirus (such as Ebola virus; EBOV) infection. To overcome this limitation in our biodefense preparedness, we have designed monoclonal antibodies (mAbs) which could be used in humans as immunoprotectants for EBOV, starting with a murine mAb (13F6) that recognizes the heavily glycosylated mucin-like domain of the virion-attached glycoprotein (GP). Point mutations were introduced into the variable region of the murine mAb to remove predicted human T-cell epitopes, and the variable regions joined to human constant regions to generate a mAb (h-13F6) appropriate for development for human use. We have evaluated the efficacy of three variants of h-13F6 carrying different glycosylation patterns in a lethal mouse EBOV challenge model. The pattern of glycosylation of the various mAbs was found to correlate to level of protection, with aglycosylated h-13F6 providing the least potent efficacy (ED_{50} = 33 μg). A version with typical heterogenous mammalian glycoforms (ED_{50} = 11 μg) had similar potency to the original murine mAb. However, h-13F6 carrying complex *N*-glycosylation lacking core fucose exhibited superior potency (ED_{50} = 3 μg). Binding studies using Fcγ receptors revealed enhanced binding of nonfucosylated h-13F6 to mouse and human FcγRIII. Together the results indicate the presence of Fc *N*-glycans enhances the protective efficacy of h-13F6, and that mAbs manufactured with uniform glycosylation and a higher potency glycoform offer promise as biodefense therapeutics.

passive immunization | antibody glycosylation | antibody-dependent cellular cytotoxicity | antiviral

Ebola viruses (EBOV; family Filoviridae) are among the most virulent infectious agents known and cause acute, and frequently fatal, hemorrhagic fever in humans and nonhuman primates. It has been reported that EBOV was weaponized by the former Soviet Union (1), and natural sporadic outbreaks occur regularly causing localized high morbidity and mortality. Due to its infectiousness and the rapidity of modern travel, the potential exists for any outbreak to become an international epidemic. Currently, there are no licensed vaccines or treatments for EBOV available. Vaccines and monoclonal antibody (mAb) antivirals have been identified as priorities by the U.S. Department of Health and Human Services for protection from EBOV used in acts of bioterrorism or war.

13F6 is a murine mAb, one of four highly protective anti-EBOV glycoprotein (GP) mAbs identified at U.S. Army Medical Research Institute of Infectious Diseases (2). 13F6 recognizes the heavily glycosylated mucin-like domain of EBOV GP and was shown to provide 100% prophylactic and therapeutic protection in a mouse challenge model (2). Murine mAbs are highly immunogenic in humans, so to make a mAb immunoprotectant more appropriate for human use, in this study we have undertaken to deimmunize (3) the 13F6 variable regions and chimerize them with human IgG_1 constant regions. Whereas CDR grafting/humanization of mAbs maximizes the content of amino acids derived from other human antibody sequences, deimmunization focuses on identifying and eliminating T-cell epitopes from the variable region sequences of antibodies.

The mechanism(s) by which 13F6 protects in vivo are largely unknown. 13F6 does not neutralize in vitro, as assessed by inhibition of plaque formation, even in the presence of complement (2), suggesting an important role for Fc-mediated effector functions in in vivo protection. Although not required for classic neutralization of virus by steric hinderance, Fc glycosylation is required for killing of virus-infected cells by complement-dependent cytotoxicity (CDC) and by antibody-dependent cellular cytotoxicity (ADCC; refs. 4 and 5). CDC activity is initiated by the binding of complement protein c1q to the Fc regions of clusters of IgG bound to an infected cell displaying viral antigen. Similarly, ADCC activity is initiated by the binding of FcγRI (CD64) and FcγRIII (CD16) on the surface of polymorphonuclear cells (PMNs) or natural killer (NK) cells to the infected cell-bound IgG Fc region. With the development of altered glycosylation pathways in yeast (6), plant (7), and mammalian cell culture (8), recent studies have begun to elucidate the role of specific glycans in enabling these effector functions. For example, elimination of core fucose has been shown to dramatically improve ADCC activity in vitro and in vivo through improved affinity for FcγRIII (7–11).

Two manufacturing systems are being pursued for the EBOV immunoprotectant: traditional mammalian cell culture production in Chinese hamster ovary (CHO) cells and transient production using viral vectors (magnICON; Bayer) in *Nicotiana benthamiana* (12, 13). By using a transgenic line of *N. benthamiana* (ΔXTFT) lacking plant-specific *N*-glycan residues (14), mAbs with highly homogenous human-like glycoforms can be generated (9, 14, 15). Comparing the efficacy of h-13F6 produced aglycosylated and glycosylated in two different production systems may help identify the mechanism(s) of action and a preferred manufacturing system for continued development of the EBOV therapeutic.

Results

Glycoform on the h-13F6 mAb Produced in *Nicotiana*. The original murine 13F6 variable regions were deimmunized as described (3) and were subsequently chimerized with human constant regions to

Author contributions: L.Z., M.P., A.H., H.S., K.J.W., and G.G.O. designed research; L.Z., J.P., C.S., N.B., and D.K. performed research; H.S. contributed new reagents/analytic tools; L.Z., J.P., C.S., L.N., H.S., K.J.W., and G.G.O. analyzed data; and L.Z., C.S., N.B., D.K., M.P., A.H., L.N., H.S., K.J.W., and G.G.O. wrote the paper.

The authors declare no conflict of interest.

*This Direct Submission article had a prearranged editor.

Freely available online through the PNAS open access option.

Data deposition: The sequences reported in this paper have been deposited in the GenBank database (accession nos. JN374688 and JN374689).

[1]To whom correspondence should be addressed: E-mail: larry.zeitlin@mappbio.com.

generate h-13F6 (JN374688 and JN374689). The resulting deimmunized, chimeric mAb DNA (h-13F6) was expressed in two different systems. The first system, CHO cells, are currently the most common platform used to manufacture FDA-approved recombinant mAbs. A stable h-13F6 CHO line was used to produce the h-13F6 mAb that contained typical glycans commonly found on recombinant antibodies (Fig. 1). The second production method is a transient plant system (magnICON; refs. 12 and 16) in which the heavy and light chain genes are cloned into separate vectors containing different but compatible viral replicons to allow for the simultaneous expression of heavy and light chains from replicating viral segments. The heavy- and light-chain vectors were then introduced into *Agrobacterium tumefaciens* to allow for high efficiency infection of 1-mo-old *N. benthamiana* plants by vacuum infiltration.

In addition to the h-13F6 DNA used for expression in CHO cells or plants, we made an additional construct containing an alanine at N297 of the human IgG_1 heavy-chain constant region (h-13F6$_{agly}$) to eliminate Fc glycosylation entirely. The h13F6$_{agly}$ was produced in the plant system.

To generate h-13F6 mAb with unique glycoforms, the *N. benthamiana* plants used for *Agrobacterium* infection and subsequent antibody production was in turn modified by RNAi expression to eliminate the expression of the endogenous plant-specific xylosyl and fucosyl transferase genes (14).

To determine the glycoforms of these h-13F6 variants, mAbs were purified by Protein A affinity chromatography and subjected to *N*-glycosylation analysis using LC-ESI-MS. Rituxan, a CHO-derived FDA-approved mAb, was included as a control. The *N*-glycosylation profile of the two CHO-derived mAbs (i.e., h-13F6$_{CHO}$ and Rituxan) exhibited 3–5 glycoforms, most of them with core α1,6 fucosylation. In both cases, nongalactosylated G_0 and monogalactosylated G_1 complex *N*-glycan structures were the major glycoforms (Fig. 1). In contrast, no fucosylated structures were detected in h-13F6$_{\Delta XF}$. This variant carried a single major complex *N*-glycan species, namely GnGn corresponding to the fucose-free G_0 structures derived from CHO production (Fig. 1). As expected, no glycan structures were detected in h-13F6$_{agly}$.

Binding of h-13F6 Variants to Human Fcγ Receptors and Human c1q. Because h-13F6 is being developed for human use, we tested the ability of the variants to bind to human proteins important for IgG Fc-mediated effector functions that may contribute to the protective efficacy of the mAb.

Affinity of mAbs for FcγRI (CD64). Surface plasmon resonance was performed to determine the affinities of the h-13F6 mAbs for recombinant human FcγRI (Table 1), a receptor important for ADCC (4, 5). h-13F6$_{CHO}$ had a similar affinity to Rituxan, with the h-13F6$_{\Delta XF}$ mAb showing slightly more potent binding ($P < 0.05$). Binding by h-13F6$_{agly}$ was significantly ($P < 0.05$) lower than all of the other mAbs tested.

Table 1. Affinity of the h-13F6 mAbs for human FcγRI (CD64) and FcγRIII (CD16)

	K_D ($\times 10^{-8}$ M)	
mAb	FcγRI (CD64)	FcγRIII (CD16)
h-13F6$_{CHO}$	4.1 ± 1.2	7.1 ± 1.2
h-13F6$_{\Delta XF}$	1.6 ± 0.3	2.5 ± 0.3**
h-13F6$_{agly}$	34 ± 16	12 ± 1*
Rituxan	2.2 ± 0.7	91 ± 18

Surface plasmon resonance (Biacore) was performed using CM5 chips coated with recombinant FcγRI and FcγRIII. Values presented are the average of 3 individual experiments with SE. *$P < 0.01$ compared with h-13F6$_{CHO}$; **$P < 0.005$ compared with h-13F6$_{CHO}$.

Affinity of mAbs for FcγRIII (CD16). Surface plasmon resonance was also performed with recombinant FcγRIII (Table 1), a receptor important for induction of ADCC by NK cells (9, 10). Of the h-13F6 molecules, the aglycosylated version had the weakest affinity ($12 \pm 1.0 \times 10^{-8}$ M), with CHO ($7.1 \pm 1.2 \times 10^{-8}$ M) having slightly stronger affinity ($P < 0.01$), and h-13F6$_{\Delta XF}$ having significantly higher affinity ($2.5 \pm 0.3 \times 10^{-8}$ M; $P < 0.005$ compared with h-13F6$_{CHO}$; $P < 0.001$ compared with h-13F6$_{agly}$). Notably, these are all high affinities for what is traditionally considered a low- to medium-affinity receptor. In fact, the affinity of Rituxan was ~8-fold less than h-13F6$_{agly}$, 13-fold less than h-13F6$_{CHO}$, and 36-fold less than h-13F6$_{\Delta XF}$ ($P < 0.005$ for all comparisons).

C1q binding. C1q binding to the Fc region of antibodies, the first step in the classical complement cascade, is glycosylation dependent (4). The ability of the three different versions of h-13F6 to bind human c1q was compared (Fig. 2) using a standard ELISA (17). As expected, h-13F6$_{agly}$ did not bind c1q at the concentrations tested. In contrast, binding of both h-13F6$_{CHO}$ and the h-13F6$_{\Delta XF}$ was observed, although h-13F6$_{\Delta XF}$ was a slightly less potent binder than h-13F6$_{CHO}$ and Rituxan.

Binding of mAbs to Murine FcγRs. Because the h-13F6 mAbs were being tested in a mouse model, surface plasmon resonance was used to compare the relative binding of the mAbs to murine FcγRI, -II, and -III to support the in vivo testing (rather than to determine full kinetics for a cross-species interaction with little relevance beyond this study). With the different murine FcγRs captured on a sensor chip, a fixed concentration (5 μg/mL) of the

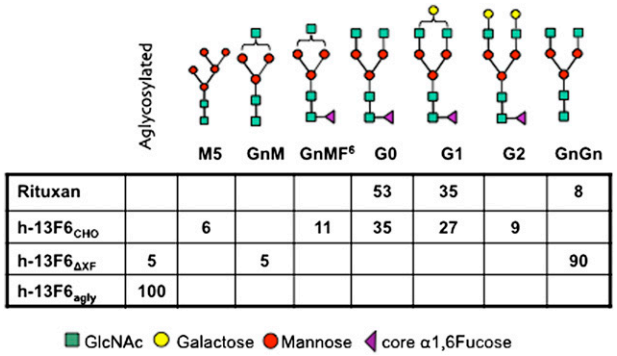

Fig. 1. *N*-glycosylation profile of different h-13F6 glycoforms and Rituxan as determined by LS-ESI-MS. Numbers represent the presence of the different glyco-species in %. Minor glycoforms (below 5%) are not indicated. *N*-glycan nomenclature according to www.proglycan.com.

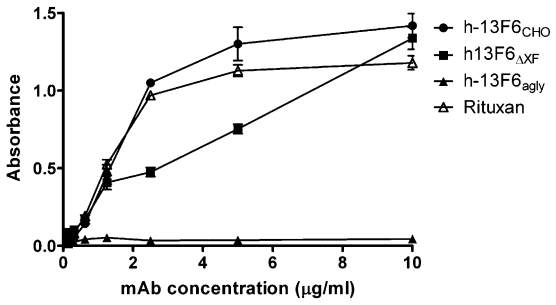

Fig. 2. C1q binding ELISA. Various concentrations of mAb were coated onto ELISA plates. After blocking, 2 μg/mL of human C1q was added. The binding of C1q to the mAb was detected using goat anti-human C1q polyclonal antibody followed with rabbit anti-goat (human adsorbed) HRP-conjugated antibody. Error bars indicate SD ($n = 3$).

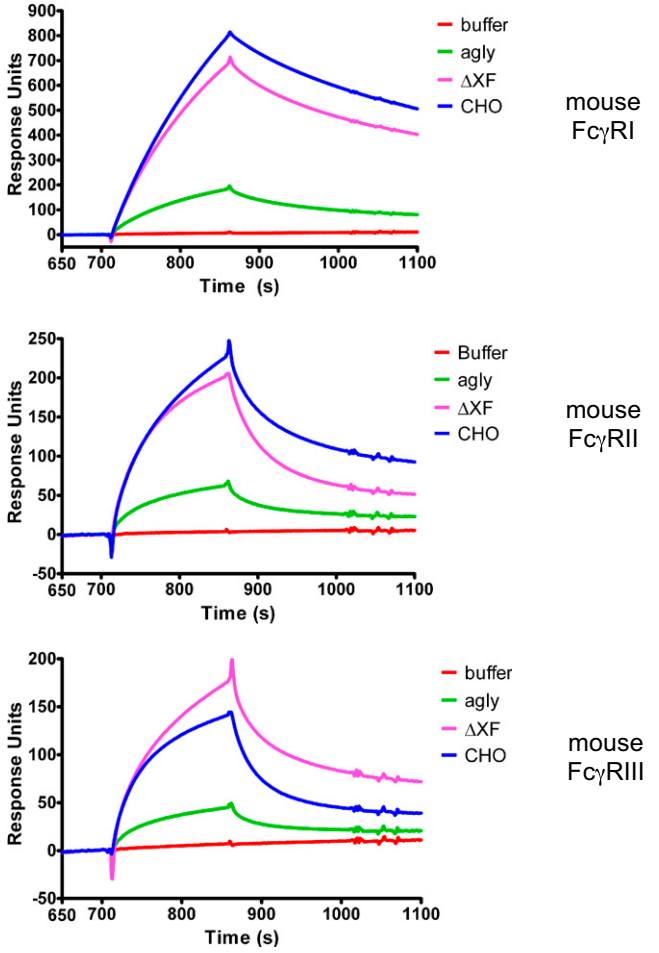

Fig. 3. Surface plasmon resonance sensorgrams showing binding and dissociation of h-13F6 mAbs to murine FcγRs. Approximately 1,000 RUs of HIS-tagged recombinant murine Fcγ receptors were bound to an NTA sensor chip. h-13F6 mAb (5 μg/mL) was subsequently flowed across the surface.

mAbs was flowed over the chip (the resulting sensorgrams are displayed in Fig. 3). h-13F6$_{CHO}$ bound better than h-13F6$_{\Delta XF}$ and h-13F6$_{agly}$ to mouse FcγRI and II, whereas h-13F6$_{\Delta XF}$ had superior binding than h-13F6$_{CHO}$ and h-13F6$_{agly}$ to mouse FcγRIII.

Efficacy of mAbs Against Lethal EBOV Challenge. To determine whether the different *N*-glycoforms present on the Fc region of these mAbs have an effect on efficacy in vivo, the h-13F6 variants were tested in a well established lethal EBOV challenge model. Groups of mice (n = 10) received single i.p. doses of mAb followed by a lethal challenge (1,000 pfu, ~30,000 LD_{50}). The resulting dose–response data are shown in Fig. 4. Although a highly lethal challenge was administered, 20% of control mice survived (Fig. 5). This observation is common because of the Institutional Animal Care and Use Committee requirement that mice displaying significant morbidity be treated with a DietGel nutritional supplement. h-13F6$_{\Delta XF}$ was more protective (ED_{50} = 3 μg ~0.15 mg/kg) than h-13F6$_{CHO}$ (ED_{50} = 11 μg, ~0.55 mg/kg). For comparison, the protection reported with the original murine 13F6 mAb is also shown (2) and suggests the deimmunization and human chimerization of the murine mAb resulted in no change in efficacy. As would be expected if the protective activity of the mAb involved any Fc-mediated effector function mechanisms, the aglycosylated h-13F6$_{agly}$ provided less protection (ED_{50} = 33 μg, ~1.65 mg/kg). Relative potency was significantly different between h-13F6$_{\Delta XF}$ and h-13F6$_{CHO}$ (relative

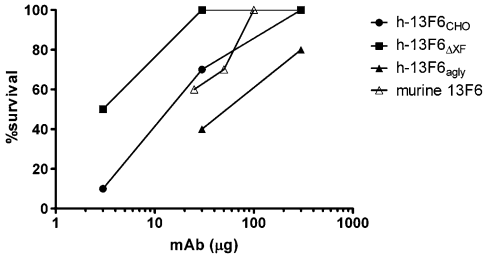

Fig. 4. Summary of dose–response experiment in mice. Mice (n = 10) received mAb i.p. 1 d before i.p. challenge with 1,000 PFU of mouse-adapted Ebola Zaire. *P < 0.05 compared with 3 μg of h-13F6$_{CHO}$ and PBS (Mantel–Cox). **P = 0.08 compared with 30 μg h-13F6$_{CHO}$; P < 0.001 compared with 30 μg of h-13F6$_{agly}$ and PBS. Murine 13F6 data obtained using identical experimental conditions are plotted from table 1 in ref. 2).

potency: 0.26, 95% confidence interval: 0.07–0.91) and between h-13F6$_{\Delta XF}$ and h-13F6$_{agly}$ (relative potency: 10.72, 95% confidence interval: 2.10–81.53).

Survival curves for the low-dose groups (3 μg, ~0.2 mg/kg) are shown in Fig. 5. Mice receiving h-13F6$_{\Delta XF}$ were significantly protected (median survival of 18.5 d) compared with h-13F6$_{CHO}$ (P < 0.05; median survival of 7 d) and the negative PBS control (P < 0.05; median survival of 6 d).

Discussion

The h-13F6 binding results for FcγRI and c1q are consistent with previous reports demonstrating that the absence of fucose does not affect the binding of IgG_1 (4, 18). Similar to other reports (8), elimination of core fucose from h-13F6 (h-13F6$_{\Delta XF}$) resulted in an improved affinity for FcγRIII. However, it is noteworthy that all versions of h-13F6 had superior affinity to FcγRIII than Rituxan, and in fact, displayed high affinity for what is typically considered a low-affinity receptor. A possible explanation for this may be the two-amino-acid difference between the heavy chain constant regions of h-13F6 and Rituxan (R214K, V215A) that may affect the conformation of the Fc region possibly resulting in improved affinity for FcγRIII. Alternatively, non-Fc amino acids may have a conformational affect on the Fc region. h-13F6 contains a rare Vλx light-chain variable region and the crystal structure for the murine parental mAb shows that the three light-chain complementarity-determining regions adopt unusual conformations distinct from Vκ and other Vλ light chains (19). Also noteworthy is the relatively high affinity of h-13F6$_{agly}$ for FcγRIII. Aglycosylated IgG is generally considered to be unable (20) or to only very weakly bind FcγRIII (21). Because 13F6 does not neutralize in vitro, the protective activity displayed by h-13F6$_{agly}$ may be attributable to low-level ADCC activity.

Our results suggest that Fc glycosylation of h-13F6 plays a significant role in the antiviral protection in the mouse EBOV

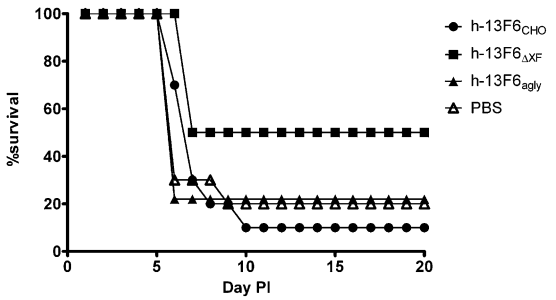

Fig. 5. Survival curves for the low-dose (3 μg) groups of mice. Data are from the groups described in Fig. 4.

model. These results are in line with a recent study that shows increased anti-lentivirus cell-mediated viral inhibition of a fucose-free anti-HIV mAb in vitro (9). Although capable of partial protection at the doses tested, h-13F6$_{agly}$ was less potent than h-13F6$_{CHO}$ with heterogenous mammalian type glycosylation. h-13F6$_{\Delta XF}$, with homogenous glycans lacking a core fucose, showed increased protection by a factor greater than twofold. Elimination of core fucose dramatically improves the ADCC activity of mAbs mediated by NK cells (8), but appears to have the opposite effect on the ADCC activity of PMNs (22). This would suggest that the improved efficacy of h-13F6$_{\Delta XF}$ may be due to ADCC mediated by NK cells via FcγRIII. Indeed, the ED_{50} for the three versions of h-13F6 are comparably ranked with the K_D of the mAbs for FcγRIII. A potential caveat when drawing conclusions from the mouse testing is that the in vivo data were generated from mAbs with human Fcγ regions interacting with mouse Fcγ receptors. However, the in vivo data are consistent with the in vitro binding data to the murine Fcγ receptors (Fig. 3), supporting the conclusion that the enhanced protection afforded by h-13F6$_{\Delta XF}$ is mediated by improved ADCC activity. In addition, the observation of equivalent protection between the original hybridoma-derived murine 13F6 and h-13F6$_{CHO}$ (Fig. 4), combined with a previous report that a chimeric mAb with IgG_1 human Fc regions can confer in vitro ADCC activity and in vivo antitumor activity comparable to its fully murine parental mAb (23), suggests that the murine Fcγ receptors may have promiscuity in binding IgG from other species similar to that reported for the murine FcRn receptor (24).

A small number of mAbs against EBOV have been found to protect in lethal mouse (2) or guinea pig challenges (25). The predictivity of these models for protection in primates is currently unknown; human mAb KZ-52 protected guinea pigs but failed to protect nonhuman primates (NHPs; ref. 26). Similarly, neutralizing polyclonal antibody also failed to protect NHPs (27). However, protection with polyclonal antibody against another filovirus, Marburg, has recently been reported (John Dye et al.; Chemical and Biological Defense Science and Technology Conference, 15–19 November 2010 in Orlando, FL), suggesting that, with the right specificity, protection against EBOV should be achievable. NHP studies will help determine the potential of h-13F6 as an EBOV virus immunoprotectant for human use.

In sum, we have focused on the role of glycosylation in the development of an immunoprotectant for Ebola virus. We engineered plants to produce an anti-EBOV mAb with a highly homogenous *N*-glycosylation profile (h-13F6$_{\Delta XF}$) carrying biantennary *N*-glycans with terminal *N*-acetylglucosamine on both branches (GnGn) and lacking potentially immunogenic plant-specific β1,2 xylose and core α1,3 fucose. The resulting glycosylation profile is considerably more uniform than typically observed in mammalian cell culture (Fig. 1). Greater homogeneity allows for more precise comparisons of the role specific glycans play in mAb functionality. Expression systems that produce recombinant mAbs from mammalian cells are typically heterogenous mixtures of glycoforms (28). Although first described over 20 y ago in transgenic *Nicotiana* (29), it is only within the last 4–5 y that rapid and high-yield production of mAbs in plants has become routine (13, 30). Manufacturing in plants offers the potential for reduced cost of goods at commercial scale and very clear cost savings during early cGMP manufacturing (31, 32). A historic concern with manufacturing therapeutics in plants has centered on the potential of plant-specific sugars to be immunogenic and change drug pharmacokinetics. However, with the development of mutants of *N. benthamiana* with human-type glycosylation (14), these concerns have been dramatically reduced, if not eliminated. Recent studies have also shown plants are capable of producing mAbs carrying *N*-glycans with terminal galactose (15) and sialic acid (33), glycans important for mAbs when Fc-mediated complement or anti-inflammatory activities, respectively, are important mechanisms of action.

Materials and Methods

***N. benthamiana* Expression Vectors.** The sequence for 13F6 (accession numbers 2QHR_H and 2QHR_L) was used by Biovation (Edinburgh, Scotland) to generate the variable regions of h-13F6 (accession number TBD – sequence submitted to GenBank 7-11-11) via proprietary peptide threading software on a fee-for-service basis. Deimmunized (3) h-13F6 murine heavy and light chain variable regions joined with human IgG_1 and lambda chain constant regions were codon optimized for expression in *N. benthamiana*. An aglycosylated version was designed by mutating the heavy chain constant region *N*-glycosylaton (N297A) site. Genes were synthesized (GeneArt) and subsequently cloned into plant (TMV and PVX) expression vectors (Icon Genetics), followed by transformation into *A. tumefaciens* strain ICF320 (30).

Production of h-13F6$_{\Delta XF}$ and h-13F6$_{agly}$ in ΔXTFT *N. benthamiana*. For transient expression of h-13F6 in planta, we used the "magnifection" procedure [Icon Genetics, Halle (Saale), Germany] as described (34), with minor modifications. Plants grown for 4 wk in an enclosed growth culture room with 20–23 °C were used for vacuum infiltration. Equal volumes of overnight-grown *Agrobacterium* cultures were mixed in the infiltration buffer (10 mM Mes, pH 5.5/10 mM $MgSO_4$), resulting in a 1:1,000 dilution for each individual culture. The infiltration solution was transferred into a 20-L custom-built vacuum chamber (Kentucky Bioprocessing, Owensboro, KY). The aerial parts of entire plants were dipped upside down into the bacterial/buffer solution. A vacuum of 0.5 bars was applied for 2 min. After infiltration, plants were returned to the growth room under standard growing conditions. Eight days after infiltration, the leaf tissue was extracted in a juicer (Green Star, Model GS-1000), using 25 mL of chilled extraction buffer (100 mM Tris/40 mM ascorbic acid/1 mM EDTA) per 100 g of green leaf tissue. The plant-derived extract was clarified by lowering the pH of the extract to pH 4.8 with 1 M phosphoric acid then readjusting it to pH 7.5 with 2 M Tris base to insolubilize plant debris, followed by centrifugation at 16,000 × *g* for 30 min. The supernatant was transferred and recentrifuged at 16,000 × *g* for an additional 30 min. The clarified extract was filtered through 0.2 μm before concentration via Minim Tangential Flow Filtration System (Pall) then 0.2 μm filtered again before loading onto 5 mL of HiTrap MabSelect SuRe (GE Healthcare) Protein A column at 2 mL/min. The column then was washed with running buffer (50 mM Hepes/100 mM NaCl, pH 7.5) and eluted with 0.1 M acetic acid (pH 3.0). The resulting eluate was neutralized to pH 7 using 2 M Tris (pH 8.0) and supplemented with Tween 80 (0.01%). The mAb solution was then polished via Q filtration (Mustang Acrodisc Q membrane; Pall), aliquoted, and stored at −80 °C until used.

Production of h-13F6$_{CHO}$. A stable CHO cell line expressing h-13F6 EBOV mAb was cultured in CD OptiCHO medium (Invitrogen) and supplemented daily with CHO Feed Bioreactor Supplement (Sigma). The CHO culture was grown in suspension using 37 °C shaker with glucose level manually monitored daily and adjusted with sterile 45% Glucose Solution (Mediatech). The culture was terminated when cell viability reached below 20%. The conditioned medium was harvested and clarified via centrifugation. The clarified 13F6$_{CHO}$ conditioned medium was filtered (0.2 μm) before concentration via Minim Tangential Flow Filtration System (Pall). The conditioned medium was concentrated 10-fold, filtered (0.2 μm), and loaded onto 1 mL of HiTrap MabSelect SuRe (GE Healthcare) Protein A column at 0.5 mL/min. The column then was washed with 1× PBS running buffer and eluted with 0.1 M acetic acid (pH 3.0). The resulting eluate was neutralized to pH 7 using 2 M Tris (pH 8.0) and buffer-exchanged against 1× PBS with 0.01% Tween 80 using Amicon Ultra (Millipore). The mAb solution was then polished via Q filtration (Sartobind Q; Sartorius), aliquoted, and stored at −80 °C until used.

All purified 13F6 mAb variants (CHO, ΔXF, agly) were fully assembled as determined by SDS/PAGE and had less than 5% aggregate as determined by HPLC-SEC.

***N*-Glycan Analysis.** *N*-glycan analysis was carried out by liquid-chromatography electrospray ionization-mass spectrometry (LC-ESI-MS) of tryptic glycopeptides (35). In short, bands that correspond to the heavy chain in a Coomassie-stained SDS/PAGEs were excised, proteins S alkylated, digested with trypsin, and subsequently analyzed by LC-ESI-MS (35).

Biacore Analyses. Recombinant human FcγRI and FcγRIII (Sino Biological, China) were immobilized onto the surface of CM5 chips (GE Healthcare) using an amine-coupling kit with a target capture level of 1,000 RUs. Each

mAb (diluted in HBS-EP+ buffer; GE Healthcare) was then flowed over the chip at five different concentrations (with the highest concentration having an *R*max between 30 and 80 RUs), and kinetic analyses using BIAEvaluation software were performed (1:1 fit). Fast flow rates and controls (including a flow cell with no receptor, and immobilized receptor with flow of buffer only) were performed to ensure against acquiring mass transfer-limited data. Binding data with HIS-tagged murine Fcγ receptors (Sino Biological) were generated using a NTA sensor chip. Briefly, ~1,000 RUs of receptor was captured on the chip followed by a flow of h-13F6 mAb at a fixed concentration (5 μg/mL).

C1q Binding ELISA. The binding of human C1q (Calbiochem, San Diego, CA) to IgG mAb was assessed as described (17). High binding Costar 96-well plates (Cambridge, MA) were coated overnight at 4 °C with various concentrations of mAb diluted in coating buffer (PBS). After blocking (PBS/2% BSA) for 1 h, 2 μg/mL of human C1q was added. The binding of C1q to the mAb was detected by using a 1/1,000 dilution of goat anti-human C1q polyclonal antibody (Calbiochem) followed with a 1/5,000 dilution of rabbit anti-goat (human adsorbed) HRP-conjugated antibody (Southern Biotech, Birmingham, AL). The plates were developed with TMB (KPL, Gaithersburg, MD). The reaction was stopped with 2.5 N H_2SO_4, and the absorbance at 450 nm was measured.

Virus, Animals, and Infections. Mouse-adapted EBOV virus was obtained from Mike Bray (36). Female C57BL/6 or BALB/c mice (5-8 wk old) were obtained from the National Cancer Institute (Frederick, MD) and housed under specific pathogen-free conditions. mAbs were delivered by i.p. injection 1 d before challenge. For infection, mice were inoculated i.p. with 1,000 PFU (30,000 LD_{50}) of mouse-adapted EBOV virus in a biosafety level 4 (BSL-4) laboratory. Animals were observed at least daily for 28 d after exposure to the virus. Research was conducted in compliance with the Animal Welfare Act and other federal statutes and regulations relating to animals and experiments involving animals, and adheres to principles stated in the Guide for the Care and Use of Laboratory Animals, National Research Council (1996). The facility where this research was conducted is fully accredited by the Association for the Assessment and Accreditation of Laboratory Animal Care International.

Statistics. Survival curves were analyzed with the log-rank (Mantel–Cox) test. Affinities were compared with an unpaired *t* test (two-sided). Logistic regression models were used to obtain the point estimate and confidence interval for ED_{50} where the dependent variable was the logit of the probability of survival, and the independent variable was the log of dose. ED_{50} was estimated by using negative of the ratio of the model's intercept to the slope (the regression estimate of the log dose). The SE of the estimated ED_{50} was calculated using the model's variance–covariance matrix of the estimated intercept and slope. Relative potency, a quantity defined as the ratio of two ED_{50} and its 95% confidence interval were estimated using logistic regression models with two intercepts, and a common slope (for the two compared assays), under the assumption of parallel lines. The estimate of the relative potency was the ratio of the difference of the two intercepts to the slope estimate. Fieller's theorem (37) was used to derive the 95% confidence interval for the relative potency estimate. All analyses were performed using Prism software (GraphPad) and SAS software (38).

ACKNOWLEDGMENTS. We thank Dr. Yuri Gleba for providing access to the magnICON expression system, Dr. Ognian Bohorov for comments on the manuscript, and Drs. Friedrich Altmann and Johannes Stadlmann for glycan analyses. This work was supported by National Institute of Allergy and Infectious Diseases Grants AI61270 and AI 72915 and Department of Defense Grant DAMD 17-02-2-0015, and partially supported by Defense Threat Reduction Agency Grant 4.10007-08-RD-B.

1. Alibek K (1999) *Biohazard: The Chilling True Story of the Largest Covert Biological Weapons Program in the World–Told from Inside by the Man Who Ran It* (Random House, New York).
2. Wilson JA, et al. (2000) Epitopes involved in antibody-mediated protection from Ebola virus. *Science* 287:1664–1666.
3. Jones TD, Crompton LJ, Carr FJ, Baker MP (2009) Deimmunization of monoclonal antibodies. *Methods Mol Biol* 525:405–423, xiv.
4. Jefferis R (2005) Glycosylation of recombinant antibody therapeutics. *Biotechnol Prog* 21:11–16.
5. Jefferis R (2009) Glycosylation as a strategy to improve antibody-based therapeutics. *Nat Rev Drug Discov* 8:226–234.
6. Li H, et al. (2006) Optimization of humanized IgGs in glycoengineered Pichia pastoris. *Nat Biotechnol* 24:210–215.
7. Cox KM, et al. (2006) Glycan optimization of a human monoclonal antibody in the aquatic plant Lemna minor. *Nat Biotechnol* 24:1591–1597.
8. Umaña P, Jean-Mairet J, Moudry R, Amstutz H, Bailey JE (1999) Engineered glycoforms of an antineuroblastoma IgG1 with optimized antibody-dependent cellular cytotoxic activity. *Nat Biotechnol* 17:176–180.
9. Forthal DN, et al. (2010) Fc-glycosylation influences Fcγ receptor binding and cell-mediated anti-HIV activity of monoclonal antibody 2G12. *J Immunol* 185:6876–6882.
10. Niwa R, et al. (2004) Defucosylated chimeric anti-CC chemokine receptor 4 IgG1 with enhanced antibody-dependent cellular cytotoxicity shows potent therapeutic activity to T-cell leukemia and lymphoma. *Cancer Res* 64:2127–2133.
11. Junttila TT, et al. (2010) Superior in vivo efficacy of afucosylated trastuzumab in the treatment of HER2-amplified breast cancer. *Cancer Res* 70:4481–4489.
12. Giritch A, et al. (2006) Rapid high-yield expression of full-size IgG antibodies in plants coinfected with noncompeting viral vectors. *Proc Natl Acad Sci USA* 103: 14701–14706.
13. Hiatt A, Pauly M (2006) Monoclonal antibodies from plants: a new speed record. *Proc Natl Acad Sci USA* 103:14645–14646.
14. Strasser R, et al. (2008) Generation of glyco-engineered Nicotiana benthamiana for the production of monoclonal antibodies with a homogeneous human-like N-glycan structure. *Plant Biotechnol J* 6:392–402.
15. Strasser R, et al. (2009) Improved virus neutralization by plant-produced anti-HIV antibodies with a homogeneous beta1,4-galactosylated N-glycan profile. *J Biol Chem* 284:20479–20485.
16. Marillonnet S, et al. (2004) In planta engineering of viral RNA replicons: efficient assembly by recombination of DNA modules delivered by Agrobacterium. *Proc Natl Acad Sci USA* 101:6852–6857.
17. Idusogie EE, et al. (2001) Engineered antibodies with increased activity to recruit complement. *J Immunol* 166:2571–2575.
18. Raju TS (2008) Terminal sugars of Fc glycans influence antibody effector functions of IgGs. *Curr Opin Immunol* 20:471–478.
19. Lee JE, et al. (2008) Complex of a protective antibody with its Ebola virus GP peptide epitope: unusual features of a V lambda x light chain. *J Mol Biol* 375:202–216.
20. Sazinsky SL, et al. (2008) Aglycosylated immunoglobulin G1 variants productively engage activating Fc receptors. *Proc Natl Acad Sci USA* 105:20167–20172.
21. Shields RL, et al. (2001) High resolution mapping of the binding site on human IgG1 for Fc gamma RI, Fc gamma RII, Fc gamma RIII, and FcRn and design of IgG1 variants with improved binding to the Fc gamma R. *J Biol Chem* 276:6591–6604.
22. Peipp M, et al. (2008) Antibody fucosylation differentially impacts cytotoxicity mediated by NK and PMN effector cells. *Blood* 112:2390–2399.
23. Steplewski Z, et al. (1988) Biological activity of human-mouse IgG1, IgG2, IgG3, and IgG4 chimeric monoclonal antibodies with antitumor specificity. *Proc Natl Acad Sci USA* 85:4852–4856.
24. Ober RJ, Radu CG, Ghetie V, Ward ES (2001) Differences in promiscuity for antibody-FcRn interactions across species: implications for therapeutic antibodies. *Int Immunol* 13:1551–1559.
25. Parren PW, Geisbert TW, Maruyama T, Jahrling PB, Burton DR (2002) Pre- and post-exposure prophylaxis of Ebola virus infection in an animal model by passive transfer of a neutralizing human antibody. *J Virol* 76:6408–6412.
26. Oswald WB, et al. (2007) Neutralizing antibody fails to impact the course of Ebola virus infection in monkeys. *PLoS Pathog* 3:e9.
27. Jahrling PB, Geisbert JB, Swearengen JR, Larsen T, Geisbert TW (2007) Ebola hemorrhagic fever: evaluation of passive immunotherapy in nonhuman primates. *J Infect Dis* 196(Suppl 2):S400–S403.
28. Kanda Y, et al. (2007) Comparison of biological activity among nonfucosylated therapeutic IgG1 antibodies with three different N-linked Fc oligosaccharides: the high-mannose, hybrid, and complex types. *Glycobiology* 17:104–118.
29. Hiatt A, Cafferkey R, Bowdish K (1989) Production of antibodies in transgenic plants. *Nature* 342:76–78.
30. Bendandi M, et al. (2010) Rapid, high-yield production in plants of individualized idiotype vaccines for non-Hodgkin's lymphoma. *Ann Oncol* 21:2420–2427.
31. Davies HM (2010) Review article: commercialization of whole-plant systems for biomanufacturing of protein products: evolution and prospects. *Plant Biotechnol J* 8: 845–861.
32. Pogue GP, et al. (2010) Production of pharmaceutical-grade recombinant aprotinin and a monoclonal antibody product using plant-based transient expression systems. *Plant Biotechnol J* 8:638–654.
33. Castilho A, et al. (2010) In planta protein sialylation through overexpression of the respective mammalian pathway. *J Biol Chem* 285:15923–15930.
34. Marillonnet S, Thoeringer C, Kandzia R, Klimyuk V, Gleba Y (2005) Systemic Agrobacterium tumefaciens-mediated transfection of viral replicons for efficient transient expression in plants. *Nat Biotechnol* 23:718–723.
35. Stadlmann J, Pabst M, Kolarich D, Kunert R, Altmann F (2008) Analysis of immunoglobulin glycosylation by LC-ESI-MS of glycopeptides and oligosaccharides. *Proteomics* 8:2858–2871.
36. Bray M, Davis K, Geisbert T, Schmaljohn C, Huggins J (1998) A mouse model for evaluation of prophylaxis and therapy of Ebola hemorrhagic fever. *J Infect Dis* 178: 651–661.
37. Zerbe GO (1978) On Fieller's theorem and the general linear model. *Am Stat* 32: 103–105.
38. SAS Institute Inc (2003) SAS/STAT Software, Version 8, Cary NC.